

Supplementary Material for MoiréTag: Angular Measurement and Tracking with a Passive Marker

SIMENG QIU, King Abdullah University of Science and Technology, Saudi Arabia

HADI AMATA, King Abdullah University of Science and Technology, Saudi Arabia

WOLFGANG HEIDRICH, King Abdullah University of Science and Technology, Saudi Arabia

ACM Reference Format:

Simeng Qiu, Hadi Amata, and Wolfgang Heidrich. 2023. Supplementary Material for MoiréTag: Angular Measurement and Tracking with a Passive Marker. 1, 1 (May 2023), 3 pages. <https://doi.org/10.1145/3588432.3591538>

A VALIDATION

We demonstrate the effectiveness of our validation approach in Fig. 1 by using four examples of captured images, each row is taken at different distances ranging from 1 - 4 meters. We first capture the initial viewing angle θ_0 , and continued the process by incrementally rotating the rotation stage by $\Delta\theta = 1^\circ$ to capture additional angles. After that, we utilize an MLP model to estimate the angle of each image and calculate the difference with the initial viewing angle of θ_0 for precision analysis. It should be taken into consideration that detecting QR finder patterns becomes increasingly challenging when capturing images at a distance close to 4 m and at a large angle, resulting in a limited maximum angular range of approximately 50° near this distance.

The first line of Fig. 2 shows the phase distribution of each Moiré pair. The actual phase value of each edge point describes the repetitive character and range of each Moiré pair. The corresponding angular range of each Moiré pair is from -65° to 65° . To further illustrate the stability of the training dataset, we plot the trends of each Moiré pair's training dataset in the second row. To assess the stability of our MLP model, we capture a total of 203 angular images 40 times and plot the phase values of each image's extracted Moiré pattern across a wide angular range. The x-axis of each figure represents the 8120 training dataset. The phase trends of each Moiré pair in the figures are similar to the phase distribution in the first row, providing further evidence of the model's stability.

B HYPERBOLIC CHIP

Fig. 3 (a) illustrates the conception of our derived hyperbolic chirp model. The hyperbolic model is derived from two similar triangles colored in yellow lines on the right image. In Figure 3 (b), an example of the hyperbolic chirp is shown. We attach the MoiréTag to the middle of a rotation stage and turned clockwise at a relatively large angle of 49.88° . The resulting pattern is captured and the horizontal Moiré pattern is extracted. Each Moiré pair's skyline is then fit to the hyperbolic period function, resulting in a red curve for each skyline with increasing frequencies from left to right. We provide more examples in different capturing distances in Figure 5. The distance approximation and focal length are shown in Figure 4 (see the supplemental video).

Authors' addresses: Simeng Qiu, King Abdullah University of Science and Technology, Saudi Arabia; Hadi Amata, King Abdullah University of Science and Technology, Saudi Arabia; Wolfgang Heidrich, King Abdullah University of Science and Technology, Saudi Arabia.

Permission to make digital or hard copies of all or part of this work for personal or classroom use is granted without fee provided that copies are not made or distributed for profit or commercial advantage and that copies bear this notice and the full citation on the first page. Copyrights for components of this work owned by others than ACM must be honored. Abstracting with credit is permitted. To copy otherwise, or republish, to post on servers or to redistribute to lists, requires prior specific permission and/or a fee. Request permissions from permissions@acm.org.

© 2023 Association for Computing Machinery.

XXXX-XXXX/2023/5-ART

<https://doi.org/10.1145/3588432.3591538>

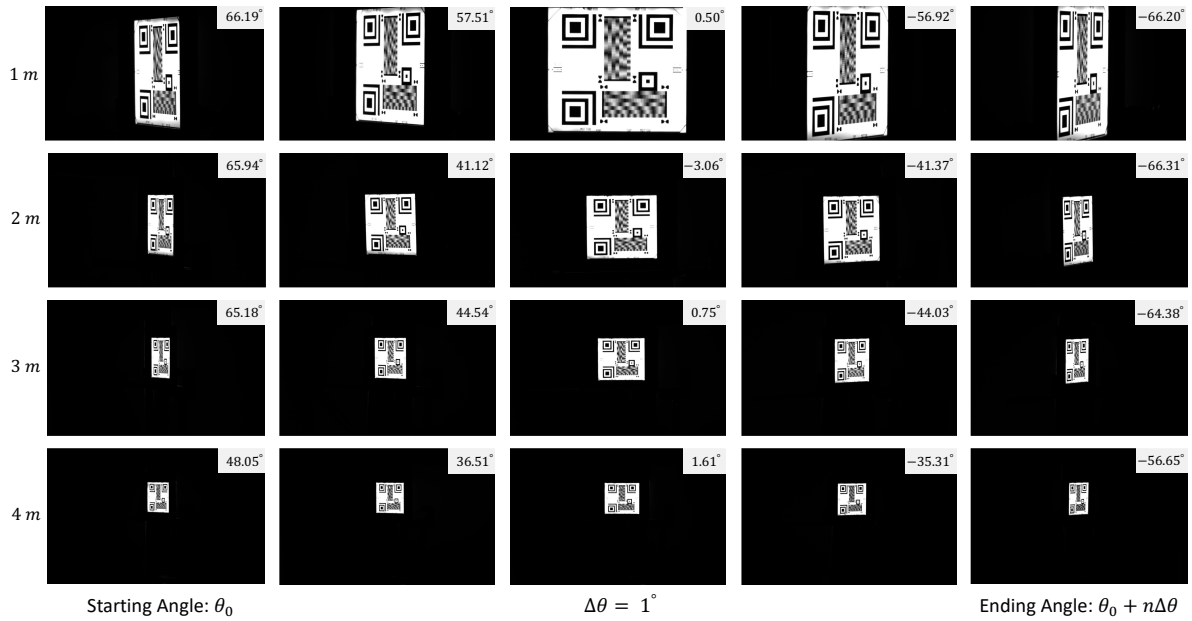


Fig. 1. *Validation Results.* We provide four examples of validation, where images were captured at distances ranging from 1 to 4 meters. When capturing at a distance around 4 meters, a limited maximum angular range may occur due to the QR finder patterns.

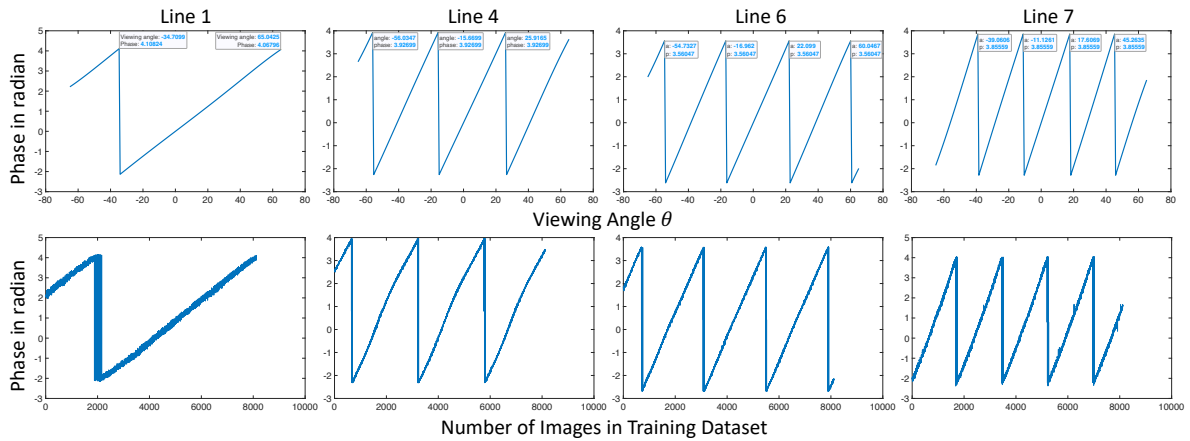


Fig. 2. The first row shows the phase distribution of each Moiré pair captured over a wide angular range. The second row demonstrates the stability of the training dataset.

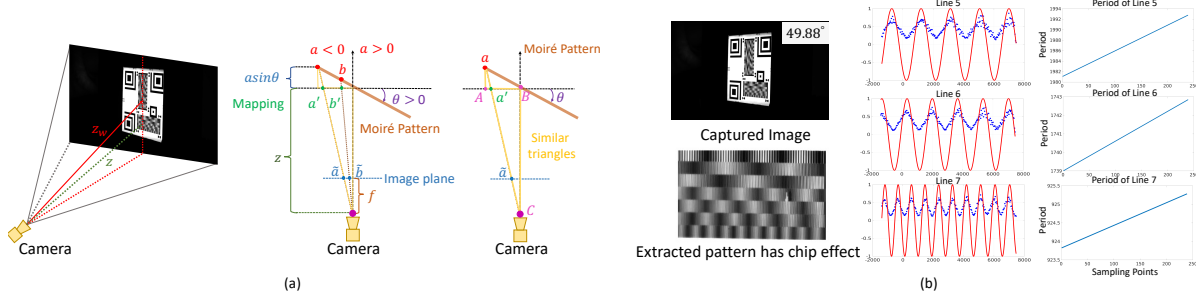


Fig. 3. (a) Hyperbolic chirp model. The orange line in the middle image represents the horizontal Moiré pattern’s top view. When the line is overlap with the horizontal axis, viewing angle $\theta = 0$. Viewing angle θ becomes positive when the orange line tilts clockwise, and vice versa. The coordinate points a and b are negative when sitting on the left side of the line. (b) Example of a hyperbolic chirp. We capture the MoiréTag and extract the horizontal Moiré pattern at 49.88° . Each Moiré pair’s skyline is then fit to the hyperbolic period function, resulting in a red curve for each skyline with increasing frequencies from left to right. The designed grated periods of Line 5, 6, and 7 are 1984, 1740, and 924, respectively. By considering chirp, the real captured pattern’s period is increasing from left to right.

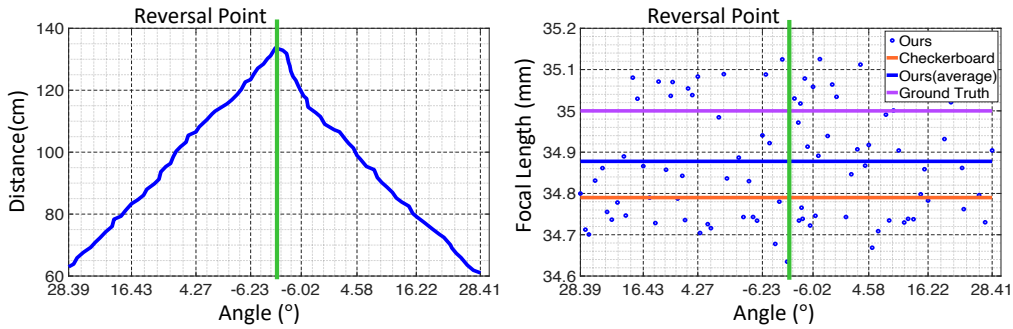


Fig. 4. Hyperbolic chirp: Distance approximation and average accuracy of focal length.

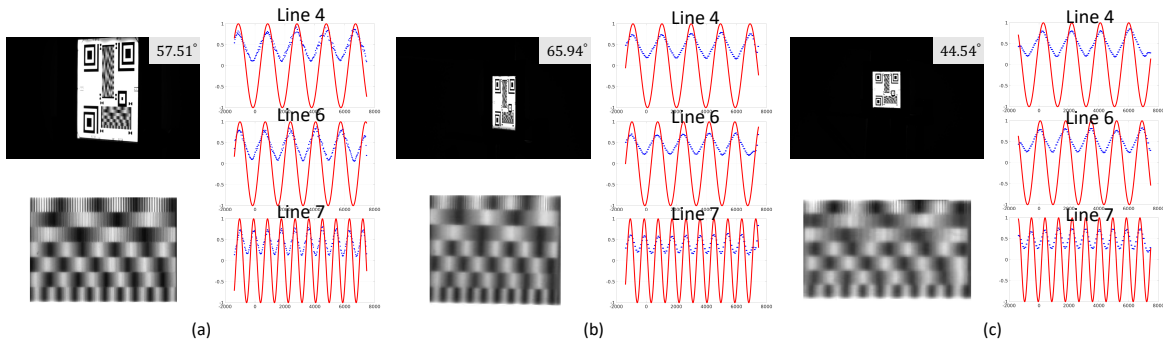


Fig. 5. We present three examples of hyperbolic chirp, along with their extracted patterns demonstrating the chirp effect, and the corresponding fitting results. The example on the left was captured at a distance around 1 meter, the one in the middle at approximately 2 meters, and the example on the right at approximately 3 meters.